JOURNAL OF PROPULSION AND POWER
Vol. 15, No. 6, November–December 1999

Unsteady Burning of Solid Propellants

Oleg Ya. Romanov*
Baltic State Technical University, 198005, Saint Petersburg, Russia

The application of methods of automatic control theory to the study of solid-propellant unsteady burning rate is described. On the basis of measurements of solid-propellant mass burning rate, by the frequency method under unsteady conditions, the necessary experimental data for identification of functional models are obtained. The results of functional modeling are used to solve unsteady combustion linear theory problems and to account for the nonlinear effects of great variations of external parameters.

Nomenclature

$A(\omega)$ = amplitude frequency response function (FRF), dimensionless
$\hat{A}$ = amplitude of pressure oscillations, dimensionless
$\hat{A}_i$ = dimensionless parameter
$\grave{A}$, $A(\tau)$ = amplitude of oscillations of unsteady burning rate, dimensionless
a = $\lambda/c\rho$ = thermal diffusivity, m^2/s
a_i = dynamic parameters of linear response function (RF), dimensionless
b_i = dimensionless parameter
C_i = dimensionless parameter
c = specific heat, kJ/kg · K
c_i = dimensionless parameter
c-phase = condensed phase in solid-propellant burning model
D_i = dimensionless parameter
d_i = dimensionless parameter
F_* = area of nozzle throat, m^2
$F(v_n)$ = nonlinear function in Eq. (47), dimensionless
$F(\tau)$ = function in Eq. (25), dimensionless
f = $\equiv \partial T/\partial x$ = temperature gradient, K/cm
f_n = nozzle throat area deviation, dimensionless
$f(t)$ = function of a time in automatic control system (ACS) dynamic equation (37)
$G(\sigma)$ = function of parameter σ, dimensionless
$G(\tau)$ = function of a time in Eq. (25), dimensionless
g = first dynamic parameter for consideration of nonlinear effect in RF, dimensionless
g-phase = gas phase in solid-propellant burning model
H = parameter, dimensionless
h = second dynamic parameter for consideration of nonlinear effect in RF, dimensionless
h_i = coefficients, dimensionless
$h(\tau)$ = transfer function, dimensionless
Im = imaginary part of complex function
j = $\sqrt{-1}$
K = parameter, dimensionless
$L(\omega)$ = amplitude FRF, dB
l = thickness of chemical reaction zone of condensed phase in solid-propellant burning model, m
m = mass burning rate, $kg/m^2 \cdot s$
n_u, n_λ, n_ω = coefficients to considerate amendments to an aperiodic part, fading decrement, and frequency oscillations of unsteady burning rate in nonlinear process, dimensionless
P = pressure, MPa
p = Laplace operator, dimensionless; also derivative operator in automatic control theory (ACT), s^{-1}
Q = heat release of generalized chemical reaction, kJ/kg
$Q(p)$ = first operational polynomial in ACS dynamic equation (37)
q = energy flux intensity, kW/m^2
q, q' = harmonic linearization coefficients
R = universal gas constant, 8.31 J/mol K
Re = real part of complex function
$R(p)$ = second operational polynomial in ACS dynamic equation (37)
r = $(\partial T_{S0}/\partial T_H)_{P_0}$
r-zone = chemical reaction zone of condensed phase
S = area of burning surface, m^2
$S(p)$ = operational polynomial for $f(t)$, Eq. (37)
s_n = deviation in area of burning surface, dimensionless
T = temperature, K
T_H = initial sample temperature, K
t = time coordinate, s
u = linear burning rate, m/s
V = combustion chamber volume, m^3
v = $u/u_0 = m/m_0$, burning rate, dimensionless
W = response function, dimensionless
$w()$ = mass reaction rate, kg/m^3 s
x = space coordinate, m
$x(t)$ = linear part in ACS dynamic equation (37)
y_n = density deviation, dimensionless
$y(t)$ = nonlinear part in ACS dynamic equation (37)
Z = $d\ell n\,\Gamma_0/d\ell n\,P_0$
$Z(t)$ = small function in time, Eq. (38)
α_c = relative concentration of in condensed phase in solid-propellant burning model, dimensionless
β_c = relative concentration of reaction product in c-phase, dimensionless
β_g = relative concentration of initial substance in g-phase reaction, dimensionless
Γ = $\sqrt{(k)}[2/(k+1)]^{(k+1)/2(k-1)}$
γ_g = relative concentration of reaction product in g-phase, dimensionless
δ = $\nu_p r - \mu k$
ε = small parameter, dimensionless
ε_i = parameter, dimensionless
η = P/P_0 = pressure, dimensionless
θ = $(T - T_H)/(T_{S0} - T_H)$, temperature, dimensionless
ϑ = $T/T_0 - 1$, temperature disturbance in combustion chamber, dimensionless
λ_d = fading decrement in oscillations of nonburning rate, s^{-1}
λ_c, λ_g = thermal conductivity in c-phase and g-phase, J/(m · s · K)
μ = $(\partial T_{S0}/\partial \ell n\,P_0)/(T_{S0} - T_H)$

Received 4 February 1998; revision received 19 May 1999; accepted for publication 31 May 1999.

*Chief, Space Vehicles and Motors Department, and Professor.

ν_p = $(\partial \ln u_0/\partial \ln P_0)_{T_H}$
ν_r = $(\partial \ln u_0/\partial \ln q_{r0})_{T_H}$
ξ = $u_0 x/a$, dimensionless space coordinate; also, λ/ω_0, relative fading coefficient, dimensionless
ρ = density, kg/m^3
σ = $\sqrt{(p+\frac{1}{4})}-\frac{1}{2}$
τ = $u_0^2 t/a$, dimensionless time coordinate
$\Phi(t)$ = small function in time
$\varphi(\omega)$ = phase FRF, dimensionless
χ = $V_0 u_0^2/\Gamma F_* a\sqrt{(\psi_0 R T_f)} = P_0 V_0 u_0^2/\rho_c S_0 \psi_0 R T_f a$
$\Psi(t)$ = oscillation phase in time, rad
$\psi(P, u)$ = diabatic coefficient, dimensionless
ψ_p = $(\partial \ln \psi_0/\partial \ln P_0)_{u0}$
ψ_u = $(\partial \ln \psi_0/\partial \ln u_0)_{P_0}$
Ω = dimensionless circular frequency of oscillations of free burning rate
ω = external-factor driven circular frequency of burning-rate oscillations, dimensionless
ω_d = external-factor driven circular frequency of burning-rate oscillations, rad/s
ω_0 = $\sqrt{(\Omega^2+\lambda^2)}$ = own circular frequency of burning-rate oscillations, dimensionless

Subscripts and Superscripts

c = condensed phase or c-phase
f = flame
g = gas phase or g-phase
i = initial
i = 1, 2, 3 . . . -counter
k = combustion chamber
l = r-zone boundary in c-phase
n = unsteady part
p = pressure
q = quasi-steady value
r = external radiant flux
s = burning surface
u = burning rate
y = steady limit
0 = base stationary value
$*$ = resonance or critical values
$\sim$ = value, dB
– = Laplace indicator

I. Introduction

MODELING the unsteady burning of solid propellants (SPs) is based on a steady combustion mechanism and quantitative data obtained from experiments in which external factors, such as pressure, radiant flux, and initial sample temperature, were kept constant. The complex nature of the burning zone is reflected only partially in unsteady models because of difficulties in describing it mathematically as well as incomplete data on the process of chemical decomposition and combustion of components, interphase interaction, and three-dimensional heat and mass transfer.

The biggest efforts have been given to models based on the assumption of one-dimensional propagation of the burning wave and the quasi-steady nature of processes taking place in the conventional gas phase (g-phase) adjacent to the sample burning surface. This assumption is, to a considerable degree, met by homogeneous SPs [double-base (DB) propellants] if one neglects the phenomena of clearly three-dimensional and unsteady character arising from the presence of a surface carbon-frame layer, the thickness of which varies over time because it is eroded by the gaseous products flowing over it. Such phenomena are characteristic of the modern SPs that contain various additives to the high-molecular mixture of the main components.

The aforementioned assumptions also can be used with high accuracy when investigating the burning of composite SPs in the range of parameters when the dispersion of the main components ensures a combustion regime in the g-phase characteristic of premixed gases. A more complex problem takes place when similar models are used to describe combustion processes of SPs based on ammonium perchlorate (AP). These propellants contain large fractions of oxidizer particles, which expand the range of parametric variation where the burning rate is limited by diffusion processes in the g-phase. The same problem is true for modern composite SPs with high-energy additives containing microdispersed aluminum, which tend to accumulate and form agglomerates of metal particles on the surface carbon-frame layer, discharge agglomerates and condensed particles into the g-phase, and burn and interact in the moving interacting dispersed environment.

Thus, we can conclude that the use of linear models with a quasi-steady g-phase assumes the averaging of parameters in the plane perpendicular to the direction of the combustion wave movement, and disregards local and microscopic effects. For this reason, the data that are obtained experimentally and that are necessary for calculating the unsteady burning rate should be generalized, and the presentation of experimental data should correspond to the burning-zone structures used in the models that only conventionally reflect the real picture. Such conventions can include the flat surface of the burning sample, the temperature and concentration of the substance on it, the kinetic parameters of chemical reactions in the condensed phase (c-phase) and the g-phase, related thermal effects, duration of particular stages of the process, and so on.

The models of SP unsteady burning described in Russian and foreign sources differ by degree of generalization and universality. Historically, a model by Zeldovich[1] initiated a family of so-called phenomenological models developed by Russian scientists in which the key position is occupied by the model of Novozhilov.[2] The approach taken in this paper accounts for inertia of the heated c-phase layer and provides for use of the steady-state functions $u(P, T_H)$ and $T_s(P, T_H)$.

Inertia of the entire c-phase is accounted for in the model presented in Ref. 3, which is constructed on the same principle. A pioneering work in which the kinetics of homogeneous chemical reactions of the c-phase and the g-phase occur over a narrow reaction zone (r-zone) was presented by Denison and Baum.[4] That model was detailed and clarified in a number of subsequent publications by Russian and foreign researchers. Summerfield and his coworkers proposed models with distributed heat release in the g-phase, in keeping with the experimentally determined law that the complex transformation of a substance is controlled by both chemical kinetics and diffusion.[5] In those models, the calculations included the averaging of parameters in planes perpendicular to the main direction of the combustion wave movement. In a generalized model, DeLuca[6] describes the most frequently used heat-release distribution along the coordinate in the g-phase with the help of three parameters found by analysis of experimental data. Reference 6 contains references to various literature sources. Such an approach can be considered phenomenological to a certain degree.

The preceding main directions of investigation of SP unsteady burning suggest that some specific concepts of burning-zone specific concepts structure should be used. Corresponding models fall into the class of structural models. Their main shortcoming, as mentioned earlier, is that the layout of the burning zone is simplified relative to the actual process.

Along with structural modeling, experimental methods can be used to obtain data on the dynamic properties of unsteady burning of SPs.[7] They help to build functional mathematical models that can play an independent role in resolving a wide range of unsteady-burning problems as well as serve as a base for further correction of the structural models, thus more completely coordinating theoretical and experimental data.[8]

Direct measurements of propellant unsteady burning rate with time-varying external stimuli allow us to create the database needed for identification of the burning zone and construction of the transfer functions (TFs) or the frequency response function (FRF). Experimental data are expanded considerably by indirect determinations of burning-rate instantaneous values as well, but acceptable mathematical models are required for the processes running in experimental setups.

The propellant burning zone can be thought of as a complex multidimensional automatic control system with several inputs and outputs. Generally, various external factors, including, for example, initial temperature, external radiant flux, relative deformation, and mass velocity of tangential flow, can be input. As external output signals, we can consider, for example, burning rate and flame temperature, burning-surface temperature, and energy flux into the c-phase, depending on the assigned problem. With linear approximation the connections between inputs and outputs can be established with the help of TF or FRF systems presented in matrix form.

Because the state of the burning zone at any instant is determined by disturbances of temperature profiles, component concentrations, and changes in its rheological properties with time, the given automatic control system has an infinite number of degrees of freedom and falls into the class of distributed parameters. In that case, the TFs contain transcendent and irrational expressions in a form that can be taken from theoretical concepts if necessary.

Finding the relation between arbitrary input signals and outputs of the automatic control system, on the basis of limited experimental investigation (object identification), assumes the availability of a certain database obtained directly and indirectly, as well as approximation in a form fit for generalization.

The most expedient is a mathematical concept in a form coupled with the results of phenomenological theory of propellant unsteady burning. In that case, it is convenient to analyze the reasons for possible disagreement between theory and experiment, so as to most effectively carry out theoretical constructions on the basis of available experimental material.

Approximation leads to mathematical representation of a functional model that helps to set up the given connection within some range of parameters. As applied to unsteady burning, it is most convenient to use FRFs or response of burning rate to a standard determinate external effect.

II. Experimental Technique

To obtain the required experimental data, it is necessary to measure the burning rate with a time resolution of at least a factor of 10 higher than the value $1/t_0 = u_0^2/a$. This corresponds to isolation of the unsteady burning low-frequency component connected to the inertia of the heated c-phase layer that has the greatest relaxation-time value. The unsteady component of the burning rate is also subject to a determination of the instantaneous burning-rate deviations from quasi-steady values, but now only by an order of magnitude less than the corresponding quasi-steady values.

Among the techniques that answer such requirements for measurements of burning rates are optical ones (high-speed filming and photo recording with self- and external illumination light) as well as techniques based on measurements of instantaneous mass and thrust created by the products flowing away from the burning surface. A special place is occupied by a burning-rate measurement technique that resolves an inverse problem of internal ballistics for SP combustion in a semiclosed volume (combustion chamber).

All of the preceding techniques require additional study because of their methodical errors. For optical techniques, it is a solution to the problem of disturbances in the area of the sample and transparent window contact[9] or close to the side surface in the case of blowing off.[10] In the determination of instantaneous sample mass, it is necessary to establish the effect of thrust on measurement results.[11] If thrust is being measured, the main task is to find a way to transform that value into a burning-rate value.[12] Finally, in the indirect determination of burning rate by resolution of an inverse problem of internal ballistics, in which the burning rate is derived from the experimental pressure-time curve, the difficulty is with an incorrectly formulated problem with corresponding consequences in accuracy of results.

The preferred experimental technique for constructing functional models is sample current mass determination.

A frequency method,[11] which has small error in measurements and high time resolution, was proposed for measuring the mass burning rate of SP unsteady burning. The method is based on SP sample mass measurement using an electromechanical frequency converter and computerized measuring instruments commonly used in frequency-control sensors.

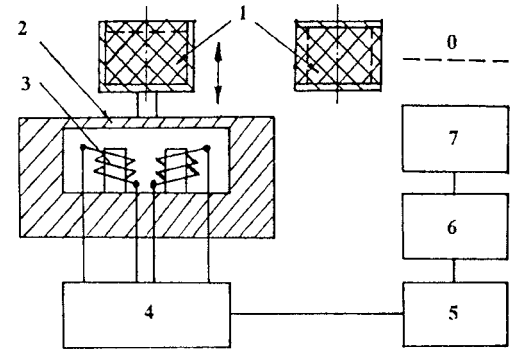

Fig. 1 Schematic of the device for measurement of SP mass burning rate by the frequency method. 1, SP sample; 2, elastic steel plate; 3, electromagnetic coils; 4, amplifier-exciter; 5, computerized frequency meter; 6, code converter; and 7, light-beam oscillograph.

A block diagram is shown in Fig. 1. With burning of an SP sample (1) fixed on an elastic steel plate (2), its mass diminishes. This results in an increase in the natural mechanical vibrations of the system performing self-sustained oscillations under the effect of disturbances produced by electromagnetic coils (3) connected with the amplifier-exciter (4). The direction of the oscillations is indicated by double-ended arrows. The frequency-modulated signal from the amplifier-exciter comes into the computerized frequency meter (5) and the numerical results of the measurements from the frequency meter output are recorded through the code converter (6) on the light-beam oscillograph (7) or can be fed directly into a computer.

The system sensitivity to sample mass changes was 4000 units of numerical variation for 1 g of burned propellant, when a frequency meter with carrier frequency of 50 MHz and an information output rate of 600 Hz were used. The sensitivity increases proportionally with a decrease in the information output rate, and vice versa. Relative error in measuring the burning rate depends on the burning-surface area, the information output rate, and the burning-rate proper. For example, for a 5-g sample with a mass decrease rate of 1 g/s and an interval between numbers of 0.01 s, the relative instrument error in measuring the burning rate is 2.5%. With an increase in mass burning rate, the error decreases correspondingly.

The effect of sample vibrations on its burning rate was investigated separately, by studying the steady-state burning rates of vibrating and steady samples. The beginning and ending times of combustion were registered with a light-beam oscillograph with the help of a photodiode oriented in the burning zone. Ignition was carried out with a radiant energy source. In those experiments, no difference in steady-state burning rate of vibrating and stationary samples was registered within the range of measurement error. This was true for vibrations directed along the burning surface and normal to it. In the latter case, the thrust acting in the vibration direction did not affect the results of mass measurements within the error range. This was proved by changing the direction of gravitational force for a sample of 0.05 N in weight, which was done by rotating the converter 180 deg. In so doing, the value of the oscillation period measured to an accuracy of the sixth decimal place did not change. The thrust measured with the technique described in Ref. 12 for a sample burning at 1.5 mm/s and a burning surface area of 1 cm^2 was less by a factor of 10 than the weight of the studied sample, which gave grounds for use of that device to measure burning rates of samples that produce thrust not exceeding 0.05 N.

The bulk of the database comprises the results of measuring the mass burning rate of unsteady propellant burning with help of a frequency sensor. The burning-rate disturbances in the region of low frequencies are recorded quite confidently in the region that corresponds to the characteristic time for the portion of the burning-zone–heated c-phase layer with the most inertia. In so doing, the external effect on the burning zone is assigned in the form of either varying radiant flux or environmental pressure.

Experiments with irradiation have been carried out on samples burning at the end in a nitrogen atmosphere in a continuous-flux tank

with constant pressure at room temperature. The burning surface was subjected to irradiation. The radiant flux intensity depended on time, with either harmonic oscillations with slowly growing frequency or a constant radiant flux that was suddenly turned off, which rather accurately simulated a step-like change with time. The intensity variation range of the radiant flux was from zero to $q_{rs} = 20$ W/cm^2.

In another experiment, in which the mean value of q_r was changed with intermittent flux, it was possible to obtain the required data for extrapolation to $q_{rs} = 0$. These results were used to determine the system's own motion relative to the propellant burning zone if experimental data were available for pressure-level changes within the range of 0.1–1.2 MPa. A similar situation could be obtained by studying unsteady combustion in a transitional regime in which the constant-value radiant flux was turned off or pressure was decreased to the next lowest level. In the latter case, sample blowoff with nitrogen was not performed, and the value range of the second pressure regime was 0.1–4.6 MPa.

The experimentally used nontransparent DB propellant of the N-type ballistite containing a combustion catalyst (1% MgO) has a $u_0(P_0)$ dependence of the form

$$u_0 = 0.35P_0^{0.81} \text{ cm/s} \qquad (P_0 = 0.1\text{–}0.8 \text{ MPa})$$

$$u_0 = 0.32P_0^{0.68} \text{ cm/s} \qquad (P_0 = 0.8\text{–}3.0 \text{ MPa})$$

$$u_0 = 0.37P_0^{0.57} \text{ cm/s} \qquad (P_0 = 3.0\text{–}6.0 \text{ MPa})$$

These values were obtained with a frequency sensor.

On the whole, the measurement technique proved to be convenient because of a natural ability to discriminate between a useful signal and noise level. The first stage of signal level was performed automatically by the electromagnetic frequency converter with discrete determination of the sample current mass, which presents a primitive function for the mass burning rate measurement. The second stage involved computerized signal processing. To find the derivative of the current mass, we used third-power splines with coefficients determined by the least-squares method.

Note that, for a transitional area with decrease in external signal (pressure or light flow), we usually got about 20 discrete points of mass measurement. In that manner the representativeness of burning-rate measurements was ensured. A similar approach also was used in experiments on the effects of harmonic variations in radiant flux in which the least-squares method was used to establish the average level, amplitude, and oscillation phases. Figures 2 and 3 present some experimental data on unsteady combustion of propellants. They show the presence of an oscillating component in responses of burning rate to changes in radiant flux and pressure.

In the case of the radiant flux effect, according to harmonic law the dependence of the variations in amplitude of the unsteady burning rate on input signal frequency demonstrates a pronounced resonance.

The oscillation amplitude of the radiant flux and its average value q_{r0} have a nonlinear effect on the resonance. By extrapolating to a zero value of amplitude, it is established that with a change of

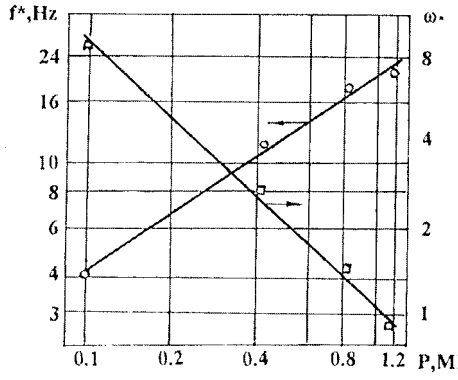

Fig. 2 Linear resonance frequency vs pressure (experimental results); f_*, ω_* = dimensional and dimensionless resonance frequencies, respectively.

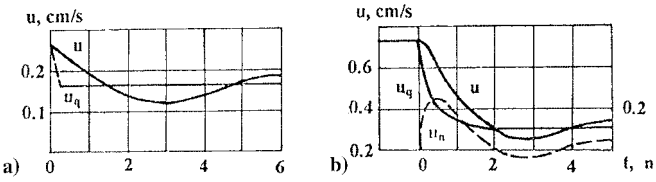

Fig. 3 Transient $u_n(t)$ regimes. a) External radiant flux is turned off, and b) pressure is decreasing to a lower regime. $u_n(t)$ has the scale in the right side of the chart.

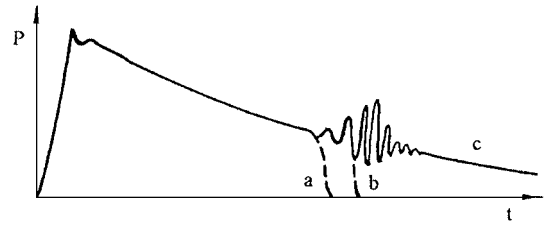

Fig. 4 Realization variants of dependence $P(t)$ in combustion chamber for slowly decreasing pressure: a = stability losses in aperiodic regime, b = stability losses in oscillatory regime, and c = stability regime is continuing. (Possible repeated regimes are not shown.)

q_{r0} the frequency grows in a manner close to that for a power law with a power index less than $2\nu_p$. That is why the resonance circular frequency ω, calculated with help of a scale, changes inversely (see Fig. 2). The value of the thermal diffusivity coefficient in calculations is taken as $a = 10^{-7}$ m^2/s.

Thus, the results of the experiments with harmonic variations in radiant flux can help us to build amplitude and phase FRFs for various q_{r0}, including its zero value. The error in amplitude and phase absolute value for burning-rate oscillations is about 6% at resonance frequency and it grows approximately as the reciprocal of the square root if those parameters decrease proportionally.

As seen in Fig. 3, and in experiments in which the external constant radiant flux is turned off or the pressure is dropping, we observe an initial time lag in burning-rate response relative to input signal in the form of the quasi-steady burning rate $u_q(t)$. Then an effect of overcontrol is manifested that can give proof of the presence of the oscillating component in corresponding TFs.

Experiments of the second type were carried out using a combustion chamber with a nozzle, where samples were burned at the end surface. The pressure was changed in two regimes: either it slowly decreased due to burnout of a plastic insert or it dropped to a lower level after a sharp increase in the throat diameter. In those experiments, measurements of both the pressure and the temperature of the combustion products were accomplished directly in front of the nozzle inlet. As a result, it was possible to indirectly determine the instantaneous propellant mass burning rate averaged over the burning surface by making use of a known internal ballistics equation and a zero-dimensional formulation with variable temperature of combustion products (numerical solution of inverse problem).

In experiments of that type with DB propellant, we used samples of composite propellant based on AP and butyl rubber with aluminum powder added (18%). The dependence of the burning rate of the second propellant on pressure has the form of $u_0 = 0.8\ P^{0.64}$ cm/s in the low pressure range of 0.1–0.8 MPa.

In the case of pressure drop in the combustion chamber, we have a picture of unsteady burning-rate behavior that agrees qualitatively with the one shown in Fig. 3. However, in cases in which the pressure decreased slowly, some nonlinear effects took place close to critical regimes, corresponding to low-frequency loss of stability in SP combustion in a semiclosed volume. Typical dependencies $P(t)$ are presented in Fig. 4a–4c. Combustion of DB propellant results in stability loss variants (a) and (b), and even in the first one, the unsteady burning rate during the pressure drop has an oscillation component that is less obvious. The composite propellant gives a picture of stability loss of (b) type or self-sustained oscillations will be damped in the process of a pressure decrease (c) with gradual

transition into a regime with subcritical escape from the nozzle. One or the other variant of system behavior is realized through pressure level, free volume, burning zone, and parameters that determine the completeness of component combustion in the chamber for each propellant.

By varying the initial conditions of the experiments, different types of pressure self-oscillation for different amplitudes and frequencies could be excited, allowing us to extrapolate the transition of unsteady burning rate to the zero level of input signal with the purpose of constructing FRFs in linear approximation. A similar approach was used in the pressure drop through variation of difference in levels of the first and second regimes.

In studying nonlinear effects, extrapolations to zero amplitude are not needed. Experiments with great deviations of unsteady burning rates from quasi-steady values allow us to find corrections to linear dependencies as functions of the deviation value.

Thus, extensive experimental data on propellant unsteady burning-rate dependencies on variable external parameters were accumulated, which comprises a necessary database for determination of FRFs and TFs.

III. Relationships for Generalization of Experimental Data

Identification of the SP burning zone as an automatic control system can be carried out by techniques developed in automatic control theory.[13] There may be a few variants for building a corresponding functional model, and some of them are tried out in the present study, for example, use of formal representations of transfer functions (TFs) with the help of inversely proportional dependencies on the complex variable, as well as Legendre's orthogonal functions in reduction of the impulse transfer function (ITF) according to the data from experiments on transition processes. However, despite the possibility of wide application of such functional models, the given direction does not contribute to discovery of internal relations in transfer functions and makes comparison with theoretical results difficult. For that reason, it seems more convenient to present transfer functions in a form that follows from structural models.

Let us examine a formulation of the unsteady combustion problem in structural modeling in which a process low-frequency component is isolated, but high-frequency ones are disregarded. A corresponding, traditionally used mechanism of SP burning zone is presented in Fig. 5. In that figure, the temperature profile throughout the entire space and the profile of the initial substance concentration in the c-phase are displayed. The profile of the substance concentration in the g-phase is not reflected because it essentially depends on what regime of burning—kinetic, diffusion, or intermediate—is realized. How deep the generalized chemical reaction in the g-phase is running, which is related to concentration, can be assessed from the distribution of heat release along the coordinate, which is determined by differentiating the dependence $T(x)$. Figure 2 also represents a linear frequency response for the cross-sectional curve of heat release intensity, which can be approximated by use of three parameters, as suggested by de Luca et al.[6] This concept reflects the most general picture of the process. In this mechanism, not only the maximum combustion temperature T_f may be meaningful, but also the maximum temperature of the first stage in the g-phase if the next temperature is realized in the afterburning regime. If that is the case, the following stage does not affect the burning rate.

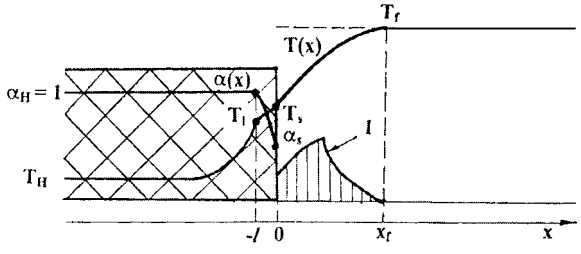

Fig. 5 Schematic of the SP burning zone (1 = qualitative sketch of volumetric heat release rate according to Ref. 6).

In the c-phase the processes are described by equations for unsteady heat and mass transfer:

$$\rho_c c_c \frac{\partial T}{\partial t} = \frac{\partial}{\partial x}\lambda_c \frac{\partial T}{\partial x} - c_c m_c \frac{\partial T}{\partial x} + Q_c W_c(\alpha, T) + q_r(x) \quad (1)$$

$$\rho_c \frac{\partial \alpha}{\partial t} = -m_c \frac{\partial \alpha}{\partial x} - W_c(\alpha, T) \quad (2)$$

with boundary conditions

$$x = 0, \qquad T = T_s(t), \qquad \alpha = \alpha_s(t)$$

$$x \to -\infty, \qquad T \to T_H, \qquad \alpha \to 1$$

$$t = 0, \qquad T = T_i(x), \qquad \alpha = \alpha_i(x) \quad (3)$$

which correspond to the generalized chemical reaction in the c-phase—≪c-phase initial substances − reaction products≫, during which $\alpha + \beta = 1$.

Because the characteristic g-phase relaxation time is much less than the relaxation time of the temperature profile in the c-phase, let us consider burning zone g-phase quasi-steady. That condition simultaneously plays the role of a low-frequency filter, which cuts off high-frequency components in unsteady processes.

Such an approach helps us to avoid formulation of general nonlinear equations for heat and mass transfer in the g-phase, which also require that interface interaction be taken into account. To achieve the assigned goal of determining the burning rate averaged by the sample cross-section, it is sufficient to maintain heat and mass balance within the burning-zone g-phase.

To simplify the procedure without narrowing the generalization of results, we assume that in dispersed particles a chemical reaction ≪c-phase initial substance − reaction product≫ with relative concentrations of α and β is in process. Immediately in the gas medium the reaction product in the c-phase but already in a gaseous state acts as an initial product. Corresponding relative concentrations β_g and γ_g follow the equation $\beta_g + \gamma_g = 1$. Besides, let us restrict ourselves to the case in which combustion proceeds under adiabatic conditions with a completed chemical reaction, and thermal parameters c_c, c_g and λ_c, λ_g are constant. Let us specify that those restrictions are only introduced to shorten the mathematical description and, if necessary, can be removed.

Then, the determination of heat, substance, and component concentration γ_g balances in the interval between the planes normal to the x axis with $x = 0$, and $x = x_f$ gives the following relations between the parameters averaged in those planes:

$$-\lambda_g f_{gs} - c_g m_g (T_f - T_s) + m_g (Q_c + Q_s)\alpha_s + m_g Q_g = 0 \quad (4)$$

$$m_c = m_g = m \quad (5)$$

$$m_g = \int_0^{x_f} w_g(\gamma_g, T)\, \mathrm{d}x \quad (6)$$

Besides, with $x = 0$ we observe continuity of heat flow, taking into account phase and chemical transformations on the c-phase surface with total thermal effect of Q_s:

$$\lambda_c f_{cs} = \lambda_g f_{gs} + m Q_s (1 - \alpha_s) + q_r(0) \quad (7)$$

Concentrations of initial substance on the surface α_s are due to physicochemical and rheological properties of the c-phase surface layer and should be designated by the relation

$$\alpha_s = \alpha_s(P, T_s, f_{cs}) \quad (8)$$

Equations (1), (2), and (4–8) with the conditions given in Eq. (3), determine seven unknown unsteady parameters α_s, T_s, f_s, f_{sg}, m, m_g, and T_f under the condition that the dependence of external effects (pressure, radiant flux, etc.) on time is assigned. Let us write a general pressure dependence:

$$P = P(t) \quad (9)$$

With inertia-free g-phase, three basic variations may occur, which are reflected in unsteady-burning phenomenological models possessing the most general features and which are of interest for searching a TF form for building a functional model. For all of them, it is justified not to carry out a detailed study of physicochemical processes of transformations in that portion of SP burning zone that is assumed to be inertia-free, but to use conclusions from relations of heat and substance balance at g-phase burning-zone borders.

In Zeldovich's[1] and Novozhilov's models[2] the r-zone of the c-phase located in the interval of $-1 \le x < 0$ is also assumed to be inertia-free, and the propellant is nontransparent. For the propellant heated layer ($x < -1$), where we can neglect the chemical reaction, Eq. (1) is written without the last two terms (shortened version), and Eq. (2) becomes confluent as $\alpha \equiv 1$. In addition to Eqs. (4–8), let us write relations of heat and mass for the c-phase r-zone:

$$-\lambda_c f_1 + \lambda_c f_s - c_c m_c (T_s - T_1) + m_c Q_c (1 - \alpha_s) = 0 \quad (10)$$

$$m(1 - \alpha_s) = \int_{-1}^{0} w(\alpha, T)\, dx \quad (11)$$

These establish relations for two additional parameters: T_1 and f_1. Further, it is assumed that $T_1 \approx T_s$, which allows us to express on the basis of Eqs. (4) and (11) each of the unknown unsteady parameters as a function of one of the others (e.g., internal temperature gradient or pressure). It is convenient to use the equations

$$m = m(f_{c1}, P), \qquad T_s = T(f_{c1}, P) \quad (12)$$

jointly with the shortened equations (1) and (9) to determine $m(t)$, $T_s(t)$, and $f_{c1}(t)$. In Zeldovich's model, it is assumed that $T_s = \text{const}$; Novozhilov's model is free of that restriction.

Because Eqs. (12), like the other similar equations related to quasi-steady g-phase, are valid to a variable extent for steady and unsteady processes, we can use, instead of Eqs. (12), the steady relations

$$m_0 = m_0(T_H, P), \qquad T_{s0} = T_{s0}(T_H, P) \quad (13)$$

In Eq. (2), a method for transformation of Eqs. (13) into Eqs. (12) is given. If one uses experimental functions (13), then data on the specific mechanism of processes in the quasi-steady portion of the SP burning zone can be neglected, and the models possess the highest level of generalization in the abovespecified assumptions.

Those assumptions have some contradiction resulting from actual identification of T_1 with T_s (see Fig. 4), which leads to a partial account for the time lag in the r-zone of the c-phase, as well as for the chemistry of the degradation processes due to variations of T_s in Novozhilov's models. It can be ascertained easily whether to continue Michelson's steady-state temperature profile in the c-phase from T_1 to T_s into the r-zone of the c-phase. However, such an approach, on the whole, improves the model quality in terms of quantitative comparison with experiments.

An exceptional merit of Novozhilov's model is its minimal mathematical description. A number of known models with concrete mechanisms and kinetics of chemical reactions in the c-phase that are based on the time-lag property of the heated c-phase layer give results that can be considered as specific cases of that model (see Ref. 2).

If so wished, it is possible to account for thermal parameters as functions of temperature and radiant flux (see Ref. 2). The losses of heat from the g-phase leading to diabatic flame also can be accounted for by introducing a corresponding correction into Eq. (13) (see Ref. 2).

In the third variant of the phenomenological model, the time-lag property of the entire c-phase in the unsteady process is taken into account.[3] Here, Eqs. (1–9) are used to determine seven unsteady parameters α_s, T_s, f_{cs}, f_{gs}, m, m_g, and T_f as functions of time. Equations (4–8) give five quasi-steady relations between them. For that reason, it is possible to isolate two parameters on which the other five depend, which are also functions of pressure. It is convenient to use the relations

$$m = m(T_s, f_{cs}, P), \qquad \alpha = \alpha_s(T_s, f_{cs}, P) \quad (14)$$

In contrast to Eq. (13), here we have not two, but three, independent values that determine the instantaneous quasi-steady distribution of parameters in the g-phase, which apparently only in a specific case may coincide with one distribution for some steady regime. Solution of Eqs. (1) and (2) together with Eq. (4) determines the profiles of concentration and temperature in the c-phase and the SP burning-zone mass rate.

As shown in Ref. 3, to find relations (14), it is possible to use the steady relations

$$m_0 = m_0(T_H, P), \qquad \alpha_{s0} = \alpha_{s0}(T_H, P) \quad (15)$$

and the heat balance equation for the steady phase,

$$\lambda_c f_{cs0} = c_c m_0 (T_{s0} - T_H) - m_0 Q_c (1 - \alpha_{s0}) \quad (16)$$

which should be considered as an implicit formulation of the functions $T_H(f_{cs0}, T_{s0})$ with constant pressure. Having taken partial derivatives with respect to f_{cs0} and T_{s0}, it is possible to describe the close vicinity of parameter variations with respect to the corresponding steady-state regime in the g-phase in the form of transforms[3]:

$$m_0(T_H, P) \to m_0(T_{s0}, f_{cs0}, P)$$

$$\alpha_{s0}(T_H, P) \to \alpha_{s0}(T_{s0}, f_{cs0}, P) \quad (17)$$

Similarly to the preceding case, it is possible to account for the effect of variable thermal coefficients in the c-phase, radiant flux, diabatic character of the flame area, and incompleteness of combustion. All of the unsteady-burning models with concrete g-phase structure and that account for time lag of the c-phase only are special cases of Romanov's model.[3] When one determines Eqs. (15) and $T_{s0}(T_H, P)$ experimentally, the data on concrete mechanism and parameters of the process in a quasi-steady g-phase are not necessary.

It should be pointed out that the concrete kinetics of the chemical reaction in the r-zone of the c-phase are still required. In particular, Romanov[3] used variants of generalized chemical reactions of the zero and first order.

Thus, unsteady-burning phenomenological models that possess a high level of generalization can serve as a base to determine the form for presentation of experimental transfer functions, which should correspond to the theoretical structure of TFs and satisfy the requirements for an optimum mathematical description. The latter provides for a decrease in the number of parameters characterizing TFs to the limit of the accuracy of experiments and any approximation. In this regard, it is convenient to compare variants of dimensionless TF structure in unsteady-burning theory and to establish general laws for its synthesis, making use of the induction principle (in our case, evolution of structure following progressive complication of the model).

In a linear approximation written with the help of TFs, the dependence for representation by the Laplace function of unsteady component of burning rate is determined by the equation

$$\overline{\nu_n} = W_p \overline{\eta_n}$$

According to phenomenological theory,[1,2] in a model with constant surface temperature T_s, two Zeldovich–Novozhilov (ZN) parameters are present (ν_p and k), and an expression for the TF written in canonical form in terms of automatic control theory will look like[8]

$$W_{p1} = \nu_p \frac{1 + \sigma}{1 + (1 - k)\sigma} \quad (18)$$

In the model with a variable, the description is carried out with four parameters (ν_p, k, r, μ):

$$W_{p2} = \nu_p \frac{(1+\sigma)(1+\delta\sigma/\nu)}{1+(1+r-k)\sigma+r\sigma^2}$$

$$= \nu_p \frac{(1+\sigma)(1+\delta\sigma/\nu)}{[1+(1-k)\sigma][1+r\sigma+rk\sigma+\cdots]} \tag{19}$$

Here, ν_p plays the role of gain factor. In the numerator and denominator, the simple multipliers appear in the form of linear and square equations, relative to σ, with 1 as a limit in decreasing p. Comparing Eqs. (18) and (19), it is possible to see the structure evolution W_p with further complication of the model. Note that the values r, μ, k should be calculated on the basis of data on the temperature of the boundary, which is taken as an interface of the r-zone and the c-phase heated layer for real systems with finite thickness of r-zone (usually this assumption is not complied with).

The presence of an irrational component in the TF shows that the burning zone is equivalent to an automatic control system with distributed parameters (it possesses an infinite number of degrees of freedom) and a result of solution of the linearized equation for unsteady heat conductivity in the c-phase heated layer, during which

$$\mathrm{Re}\sqrt{p+\tfrac{1}{4}} \geq 0, \qquad p = \sigma(\sigma+1)$$

In expression (19), it is more convenient, however, to switch to another group of parameters, having gotten rid of irrationality in the denominator:

$$W_{p2} = \nu_p \frac{1+\sigma+a_2 p+a_3 p\sigma+a_4 p^2}{1+(2\lambda p+p^2)/\omega_0^2} \tag{20}$$

where

$$\lambda = [r(k+1)-(k-1)^2]/2r^2, \qquad \omega_0 = \sqrt{k}/r$$

$$a_2 = (\delta/\nu)+[(k+r-1)/k]$$

$$a_3 = (\delta+\mu)/\nu, \qquad a_4 = \delta r/\nu k$$

i.e., λ and ω_0 are decrements of attenuation and natural frequency of burning-rate deviations. Instead of a group of parameters ν_p, r, μ, k proceeding from Eq. (20), it is convenient to take $\nu_p, \lambda, \omega_0, a_2$.

Taking into account the flame diabaticity results in the appearance of two more parameters in the burning-zone description.[2] They are important for characterizing the process as a whole, but do not change the structure of Eqs. (18–20).

In the third phenomenological model of SP unsteady burning, with completely inertial c-phase, the TF already contains at least six independent parameters.[3] In the numerator and denominator of the expression for W_{p3}, a special kind of series is included—a hypergeometric one, for a zero-order chemical reaction in the c-phase. They can be approximated in form of a truncated exponential series with respect to σ. When the condition of time-lag property of the c-phase r-zone does not change the number of denominator roots W_{p3} in the low-frequency range,[3] we obtain for TF

$$W_{p3} = \nu_p \frac{1+\psi(\sigma)}{1+(2\lambda p+p^2)/\omega_0^2} \tag{21}$$

where $\psi(\sigma)$ is the fractional rational function of σ and the $\lim \psi(\sigma) = 0$ as $\sigma \to 0$. The function $\psi(\sigma)$, in addition to ν_p, λ, ω_0, is characterized by three more independent parameters. They may be coefficients in simple multipliers grouped depending on $\psi(\sigma)$. The flame diabaticity in the given model adds two more parameters but does not affect the W_{p3} structure.

Thus, complication of the model leads to a corresponding complication of the TF structure because of the increase in a number of parameters being varied, while keeping the oscillating component from the second model [denominators in Eqs. (20) and (21)].

For uniform processing of experimental data in the case of a random change in the pressure with time in a linear approximation, it is necessary to use the known equations for ITF $k_p(\tau)$:

$$W_p(p) = \int_0^\infty k_p(\tau) e^{-p\tau}\, d\tau \tag{22}$$

$$v_n(\tau) = \int_0^\tau k_p(\tau-\xi)\eta_n(\xi)\, d\xi \tag{23}$$

The last is true for a random dependence of input signal $\eta_n(\tau)$ and zero initial data.

IV. Results of Experimental Study

In the processing of experimental data, some attempts were made to variously represent FRFs and the related ITFs. In the experiments, a condition that one variant of FRF structure fit all pressure ranges was complied with. In so doing, it was taken into account that, in transition for complex FRFs, it is sufficient in expressions for TF to substitute p for $j\omega$, first to obtain $W_p(j\omega)$ and then to obtain amplitude and phase FRFs.

First, the experiments with a radiant flux effect according to harmonic law were examined. To process them, a region of frequencies from $\omega = 0$ to ω_k was chosen that met a response amplitude equal to 20% of quasi-steady burning-rate amplitude ($\omega_k > \omega_*$). The limitation of that frequency is due to progressively increasing error following attenuation of the output signal. (With $\omega = \omega_k$ it exceeds by approximately 5 times the error typical for the resonance area.) For the same reason, the number of experimental points involved in the processing were selected more densely relative to the resonance frequency ω_*.

For an optimum mathematical description, it is expedient to gradually increase the number of parameters involved, trying to achieve the highest admissible approximation accuracy.

A typical situation occurring in the processing of experimental data is shown quantitatively in Fig. 6. With help of two-parameter approximation of the type in Eq. (18), i.e., curve 1, we can succeed only in describing the initial portion of experimental FRFs, i.e., curves 0. The use of a four-parameter approximation in form of Eq. (20), i.e., curves 2, cannot satisfy the requirements for accuracy either, since experimental FRFs do not reflect more vigorous integration of the property of transfer function as compared to experimental one. Finally, with help of a six-parameter function in form of

$$W_r = \nu_r \frac{1+a_1\sigma+a_2 p+a_3 p\sigma}{1+(2\lambda+p^2)/\omega_0^2} \tag{24}$$

which can be compared to Eq. (21), we succeed in describing experimental curves completely with sufficient accuracy. However, we may limit ourselves to five parameters in order to shorten the mathematical description, assuming that $a_3 = 0$ (curves 3). This increases the approximation error, which is more perceptible in the region of high ω. Keeping the sixth parameter a_3 in Eq. (24) makes sense when we enlarge the examined region, increasing the values of ω, and the accuracy of the experiment increases.

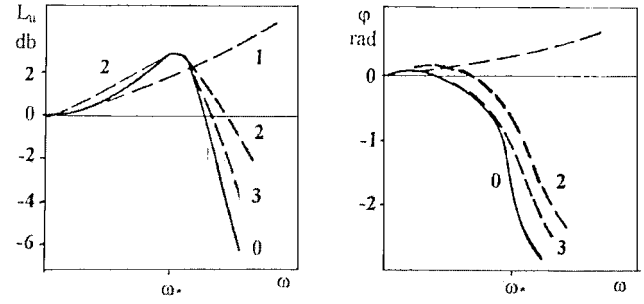

Fig. 6 Selection of approximate dependencies with various numbers of dynamic parameters.

The ITF is recovered with the help of Laplace inverse transform by Eq. (24) with $a_3 = 0$. The final expression is found by expanding into the simplest fractions with complex denominators and reducing to the relations given in Ref. 14:

$$k_r(\tau) = \nu_r e^{-\lambda\tau}\{[A_2 + C_2(b_1F - b_2G)]\sin\Omega t + [B_2 + C_2(b_2F + b_1G)]\cos\Omega t\} \tag{25}$$

where $\Omega = \sqrt{(\omega_0^2 - \lambda^2)}$ is the frequency of system free movement, and

$$b_1 = \left[\tfrac{1}{2}\sqrt{\left(\tfrac{1}{4} - \lambda\right)^2 + \Omega^2} + \tfrac{1}{4} - \lambda\right]^{\frac{1}{2}}, \qquad b_2 = \Omega/2b_1$$

$$F = \operatorname{erf}(b_1\tau) + \frac{2}{\sqrt{\pi}}e^{-b_1^2\tau}\int_0^{b_2\sqrt{\tau}} e^{y^2}\sin(2b_1\sqrt{\tau}y)\,\mathrm{d}y$$

$$G = \frac{2}{\sqrt{\pi}}e^{-b_1^2\tau}\int_0^{b_2\sqrt{\tau}} e^{y^2}\cos(2b_1\sqrt{\tau}y)\,\mathrm{d}y$$

$$A_2 = \frac{\omega_0^2}{\varepsilon}\left(1 - \frac{a_1}{2} - a_2\lambda\right)$$

$$B_2 = \omega_0^2 \cdot a_2, \qquad C_2 = 2\left(\frac{\omega_0^2}{\Omega} - A_2 - B_2\right)$$

Out of the five determining parameters, one (ν_r or ν_p) is known from the steady-state experiment; the rest were determined in dynamic regimes with an extrapolation to zero amplitude of the external stimuli. The method of random search was used. The optimum combination of parameters is in accord with a minimum rms deviation in the approximation of the transition processes and the mean relative deviations for experimental amplitude and phase FRFs.

The generalized results of the experiments are given in Table 1. It follows from the table that the natural nontransparency of a DB propellant of the given formulation makes similar the effect of radiant flux and pressure. Therefore, we can derive a unique TF

$$W_u = W_r/\nu_r = W_p/\nu_p$$

The table also presents the values of the relative attenuation coefficient $\zeta = \lambda/\omega_0$ characterizing the system steadiness factor and approximation rms error.

For the first three lines of the table, the amplitude (upper numbering) and phase FRFs corresponding to TF $W_u(j\omega)$ amplitude values in decibels are shown, $L_u = 20\log A_u(\omega)$.

In the experimental TFs, the integrating property prevails, especially in the region of high frequencies, $\omega > \omega_*$, where φ has high negative values. It is clearly reflected in a noticeable time lag of the unsteady burning rate response at the initial stages of the transitional processes for DB propellant (see Figs. 3a and 3b), when the main contribution to the value of the output signal is made by high frequencies.

Table 1 Dynamic parameters of mass burning rate of unsteady burning

P, MPa	ν_p	ν_r	λ	Ω	a_1	$-a_2$	ζ	ξ	γ, %
				DB propellant					
0.1	0.81	0.14	5.3	9.7	0.22	0.015	0.48	——	6
0.4	0.81	0.038	1.9	3.1	0.36	0.05	0.53	——	6
0.8	0.75	0.024	1.26	1.8	0.40	0.06	0.58	——	7
1.2	0.68	0.018	0.97	1.23	0.43	0.07	0.62	——	7
2.0	0.68	——	0.76	0.89	0.45	0.13	0.65	——	8
3.2	0.57	——	0.51	0.58	0.49	0.14	0.66	——	8
4.6	0.57	——	0.41	0.45	0.50	0.22	0.67	——	8
				Composite propellant					
0.1	0.64	——	1.0	1.3	0.45	0.12	——	0.77	6
0.4	0.64	——	0.82	0.96	0.52	0.15	——	0.86	7
0.8	0.64	——	0.64	0.70	0.55	0.18	——	0.91	7

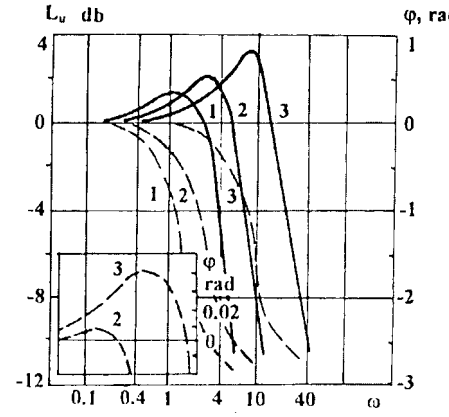

Fig. 7 Experimental amplitude and phase of FRF for pressure levels 0.8 (1), 0.4 (2), and 0.1 MPa (3).

A minor effect revealed by approximation takes place at low pressures in the low-frequency region where 0 (shown as an enlargement in the inset in Fig. 7). Let us note that the presence of a section with a leading response phase is most important in studying the steadiness limit in the combustion chamber process.

The system steadiness factor in linear approximation can be assessed primarily by its value (see Table 1). It is quite high, which is evidence of strong damping. Closer to the steadiness boundary, the propellants that are being studied are found at low pressures, where ζ is lower. A similar conclusion can be reached by examining traditional quality criteria, which usually are used for closed automatic control systems.[13]

The proposed method of identifying the SP burning zone as an automatic control system allows us to have extensive data on TFs and ITFs for concrete SPs at various levels of pressure, initial temperature, radiant flux, and so on. By generalization of the experimental results, we can arrive at the principal results of the linear theory of unsteady burning, and then, after generalization of high values of the burning-rate unsteady component, we can account for nonlinear effects as well.

V. SP Unsteady Burning Rate in Linear Approximation

The use of TF W_p with five determining parameters, that is,

$$W_p(p) = \nu_p\frac{1 + a_1\sigma + a_2 p}{1 + (2\lambda p + p^2)/\omega_0^2} \tag{26}$$

is reflected in Ref. 15.

Unsteady burning rate in linear approximation is determined by the formula derived from the Laplace transformation

$$\overline{\nu_n} = W_p(p)\overline{\eta_n} \tag{27}$$

with subsequent inverse transformation by Laplace to obtain the dependence $\nu_n(\tau)$.

A slow pressure change corresponds to a linearization of TF (26) relative to p, which results in

$$\nu_n = \nu_p\left[\eta_n + \left(a_1 + a_2 - \frac{2\lambda}{\omega_0^2}\right)\frac{\mathrm{d}\eta_n}{\mathrm{d}\tau}\right] \tag{28}$$

By replacing p with $j\omega$ (ω is the current frequency) in Eq. (26), we find the corresponding FTF, $W_p(j\omega)$. Using a Fourier inverse transform, by the same procedure we again obtain relation (28), but the operation allows us to establish the relationship of the coefficient of the derivative in Eq. (28) to the phase FRF $\varphi(\omega)$:

$$\Phi_0 = \left(\frac{\mathrm{d}\varphi}{\mathrm{d}\omega}\right)_{\omega\to 0} = a_1 + a_2 - \frac{2\lambda}{\omega_0^2}$$

Therefore, to analyze the burning-rate behavior at various steady values of pressure, it is possible to use the preceding phase FRF, which leads to the conclusion that only in a limited region of low pressure (up to 0.4 MPa) is $\Phi_0 > 0$. Here, a leading change in the propellant burning rate takes place with regard to dependence of the quasi-steady rate $v_q(\tau)$ at higher pressures, where $\Phi_0 < 0$ is the time lag.

To compare with results of the theory,[2] it is also convenient to make use of Φ_0 values. Using the ZN parameters k, r, ν_p, and μ, in a model with constant surface temperature, $\Phi_0 = k$, but in a model with variable surface temperature, $\Phi_0 = k(1 - \mu/\nu_p)$. Thus, if we wish to operate the stated parameters as formal ones for description of experimental data in the range of low frequencies, we have to assume that $k < 0$ or $\mu/\nu_p > 1$.

Let us consider the response of unsteady burning rate to a step change in the pressure. It is possible to leave out the amplitude value and operate the unit-step function of time $\eta_n = 1(\tau)$. In that case $\overline{\eta_n} = 1/p$ and a response to a unit-step effect is derived from Eq. (27) by means of the Laplace inverse transform as the TF of the automatic control system.[13]

To be formal note that a response to a step signal can be analyzed if the FTF accurately describes the system behavior at all possible frequency intervals of $0 \le \omega \le \infty$. The experimental data given above, processed in form of an approximation dependence, are valid only in the limited region of low frequencies. Therefore, the greatest error in reproducing the burning-rate response should be expected at the beginning of the transition process when the high-order frequencies prevail. (The unit-step function has, as we know, a continuous frequency spectrum.)

Let us analyze the response behavior at $\tau \ll 1$. As in Ref. 2, let us assume $p \gg 1$ in Eq. (27) and confine ourselves to the first terms of expansion. Then, after application of the Laplace inverse transform, we get

$$v_n(\tau) = \nu_p a_2 \omega_0^2 \tau \tag{29}$$

In contrast to the results in Ref. 2, the burning rate at the moment of pressure jump does not undergo a discontinuity; only a break in the derivative is observed.

Taking into account that $a_2 < 0$, we obtain for the SPs a picture that is presented qualitatively in Fig. 7: At the beginning of the transition process, the curve $v_n(\tau)$ tends to opposite behavior in the form of the step dependency $v_q(\tau)$ in relation to the input signal. Such a development of the process is the result of representing experimental data in a form that meets the minimum mathematical requirements for describing five parameters.

Let us compare that variant with a representation $W_p(p)$ described with six parameters in Eq. (24), which leads to replacement of Eq. (29) with the relation

$$v_n(\tau) = 2\nu_p a_3 \omega_0^2 \sqrt{\tau/\pi}$$

Introduction of $a_3 \neq 0$ changes to some extent the values of all of the other parameters except ν_p but provides practically no improvement in the FRF approximation accuracy, on the whole, and complicates the mathematical description. Figure 8 clearly shows how drastically the process character changes at its beginning with $a_3 > 0$ in comparison to curve 1.

If we use the Laplace inverse transform[14] in Eq. (27) with TF (26), then, with an external unit-step effect, we obtain the TF

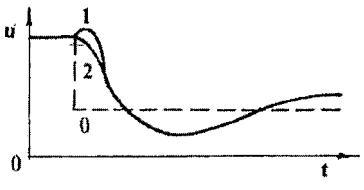

Fig. 8 Variants of the transient process initial stage for stepped external signal by approximate equations with five (1) or six (2) dynamic parameters.

$$h(\tau) = \nu_r \left\{1 - (a_1/2)\,\mathrm{erfc}(\sqrt{\tau}/2) - e^{-\lambda\tau}(C_3 \cos\Omega\tau + D_3 \sin\Omega\tau) + (a_1/\Omega)e^{-\lambda\tau}[(b_3F + b_4G)\sin\Omega\tau + (b_3G - b_4F)\cos\Omega\tau]\right\}$$

where

$$C_3 = 1 - a_1/2, \qquad D_3 = (\lambda/\Omega)(1 - a_1/2) - (a_2/\Omega)\omega_0^2$$

$$b_3 = b_2\Omega - b_1\lambda, \qquad b_4 = b_1\Omega + b_2\lambda$$

The dependence $h(\tau)$ can be assessed qualitatively in Fig. 8, as well as in the experimental curves with various pressure drops (b) in Fig. 4.

With an input signal of a random form, we have[14]

$$v_n(\tau) = \int_0^\tau h(\tau - \theta)\,\frac{\mathrm{d}\eta(\theta)}{\mathrm{d}\theta}\,\mathrm{d}\theta$$

One of the standard forms of external effect is a signal changing by the harmonic law. An expression for response (of burning rate) essentially depends on the initial signal phase. It is least complicated in the case of soft switching on, when the initial phase of the pressure following the sine curve is zero. However, even in that case the notation turns out to be very bulky, and for that reason as well as practical ones, we confine ourselves here to reduction of the undamped response portion of the steady system with input signal frequency. The unit amplitude of the input sinusoidal signal and the dimensionless cyclic frequency ω of its variation $\overline{\eta_n} = \omega/(p^2 + \omega^2)$. After substitution of $\overline{\eta_n}$ into Eq. (2) and application of the Laplace inverse transform, we obtain the following relationship describing deviations of the unsteady burning rate when the initial data are ignored:

$$v_n(\tau) = \frac{\nu_r \omega_0^2}{4\lambda^2\omega^2 + \left(\omega_0^2 - \omega^2\right)^2}[(C_4 - D_4\lambda + H)\sin\omega\tau + (\omega D_4 + K)\cos\omega\tau]$$

Here,

$$C_4 = (1 - a_1/2)\left(\omega_0^2 - \omega^2\right) + 2\lambda a_2\omega^2$$

$$D_4 = a_2\left(\omega_0^2 - \omega^2\right) - 2\lambda[1 - (a_1/2)]$$

$$H = a_1\varepsilon\left(2\lambda^2 + \omega_0^2 - \omega^2\right) - a_1\lambda\left(\omega^2/\varepsilon_1\right)$$

$$K = a_1\omega\left(2\lambda^2 + \omega_0^2 - \omega^2\right)/2\varepsilon_1 - 2a_1\varepsilon_1\lambda\omega$$

$$\varepsilon_1 = \left[\tfrac{1}{2}\left(\sqrt{\tfrac{1}{16} + \omega^2} + \tfrac{1}{4}\right)\right]^{\frac{1}{2}}$$

The amplitude of the deviation is an amplitude FRF $A_p(\omega)$ and determines the amplifying properties of the system depending on frequency and the phase, that is, the phase FRF $\varphi(\omega)$. Examples of such functions derived according to the experimental dynamic parameters for two SPs, as well as their general description, were given earlier.

VI. Stability of Steady Regime in Combustion Chamber

The problem of low-frequency stability of a steady regime in a combustion chamber leads to simultaneous consideration of equations of chamber dynamics and SP unsteady burning rate. In a zero-dimensional formulation, if combustion product parameters are averaged by free volume, then their density ρ, temperature T, and pressure P in the chamber are described by relations[16]

$$V\frac{\mathrm{d}\rho}{\mathrm{d}t} = Sm - \Gamma\frac{PF_*}{\sqrt{RT}}$$

$$V\frac{\mathrm{d}}{\mathrm{d}t}(c_v\rho T) = kmS\psi RT_f - \Gamma PF_* k\sqrt{RT}, \qquad P = \rho RT \tag{30}$$

Commensurate with the relative depth and the rate of changes of parameters during the transition process, we can assume as invariable V, Γ, R, and k, as well as the coefficient ψ determining combustion completeness in a heat-insulated chamber, and flame temperature deviations from T_f in an unsteady regime. The adequate choice of value ψ, as shown in Ref. 16, can also help to account indirectly for heat losses from a chamber without heat insulation. In both cases, we should assume that $\psi = \psi(P, u)$; thus, the given function reflects general regularity for steady and unsteady conditions. That is why it is admissible to determine it experimentally under steady conditions.

The process of combustion with constant enthalpy of equilibrium propellant-combustion products of equilibrium propellant that come from the burning surface into the chamber corresponds to $\psi = 1$; the isothermal process in the chamber corresponds to $k = 1$.

The system of equations (30) should be complemented by dependencies for unsteady burning rate and external effects (let them be the burning surface and the nozzle throat surface) as time functions:

$$u = u(P, T_H, t), \qquad S = S(t), \qquad F_* = F_*(t) \tag{31}$$

Let us introduce additional symbols for small deviations from steady-state values:

$$y_n = \rho/\rho_0 - 1, \qquad \vartheta_n = T/T_0 - 1$$

$$s_n = S/S_0 - 1, \qquad f_n = F_*/F_{*0} - 1$$

with $T_0 = \psi_0 T_f$. For definiteness, we assume the outflow regime to be above critical, that is, $\Gamma = \Gamma(k)$. After linearization of Eqs. (30) and (31) and transition to the Laplace transforms, we obtain

$$(1 - \psi_p + \chi p/k)\overline{\eta_n} - (1 + \psi_u)\overline{v_n} + \overline{\vartheta_n}/2 = \overline{s_n} - \overline{f_n}$$

$$\bar{\eta} + \chi p\overline{y_n} - \overline{v_n} - \overline{\vartheta_n}/2 = \overline{s_n} - \overline{f_n}$$

$$\overline{\eta_n} - \overline{y_n} - \overline{\vartheta_n} = 0, \qquad W_p\overline{\eta_n} - \overline{v_n} = 0 \tag{32}$$

The conclusion on steadiness is obtained by analyzing the characteristic equation, which is derived by equating the system determinant (32) to zero:

$$W_p = \nu_k \frac{1 + h_1\chi p + h_2\chi^2 p^2}{1 + h_3\chi p} \tag{33}$$

Here,

$$h_1 = \frac{(3k+1)/k - 2\psi_p}{2 - \psi_p}, \qquad h_2 = \frac{2}{k(2-\psi_p)}$$

$$h_3 = \frac{2(1+\psi_u)}{2+\psi_u}, \qquad \nu_k = \frac{2-\psi_p}{2+\psi_u}$$

The right-hand part of Eq. (33) is an expression inverse to the TF W_k of an opened system of automatic control when we consider burning rate as the input signal and pressure in the chamber as the output. We can easily make sure of the function after obvious transformations of system (32), namely, exclusion of the last equation, transposition of components containing v_n into the vector of free components, and subsequent solution.

The asymptotic, stable, steady-state combustion regimes of propellant combustion in a combustion chamber are defined by the roots of Eq. (33) with negative real components. With $p = 0$ from Eq. (33) with account of Eq. (26), we obtain a condition of static stability:

$$\nu_p < \nu_k \tag{34}$$

On the oscillating boundary of stability, we have, according to Eq. (33), the relation between FTFs,

$$W_p(j\omega) = W_k^{-1}(j\omega) \tag{35}$$

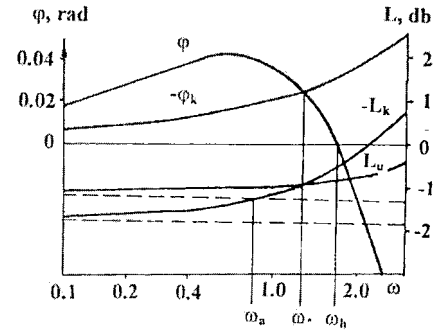

Fig. 9 Comparison of logarithmic FRFs of SP burning zone with combustion chamber showing the limit of determination of stable regime for an SP burning in combustion chamber.

which allows us to find the frequency of stability loss ω_y and the value of the instrument constant χ_* as a result of resolving the system of two equations composed of real and imaginary components, Eq. (35).

Figure 9 graphically presents an example using the experimental amplitude $L(\omega)$ and the phase $\varphi(\omega)$ FRFs of the DB propellant studied earlier, where $p = 0.1$ MPa and combustion at constant pressure is steady. Values ν_p and ν_k are converted into decibels and are plotted as the wave at the top of Fig. 9, and their levels on the graph are shown by the dashed lines; ω_* corresponds to the simultaneous intersection of $\varphi(\omega)$ and $L(\omega)$, with FRFs plotted by W_k and taken with opposite signs. With a fixed value of $\tilde{\nu}_k$, the intersection is possible in frequency range (ω_a, ω_b), where we observe an excess of L over $\tilde{\nu}_k$ and the phase φ is positive. Numerically, ω_a and ω_b are found from the conditions

$$\left(\frac{2-\psi_p}{2+\psi_u}\right)^2 = \nu_p^2 \frac{\left[(1 + a_1 \operatorname{Re}\sigma_a)^2 + (a_2\omega_a + a_1 \operatorname{Im}\sigma_a)^2\right]}{\left[\left(1 - \omega_a^2/\omega_0^2\right)^2 + 4\lambda^2\omega^2/\omega_0^4\right]}$$

$$\frac{a_2\omega_b - a_1 \operatorname{Im}\sigma_b}{1 + a_1 \operatorname{Re}\sigma_b} - \frac{2\lambda\omega_b/\omega_0^2}{1 - \omega_b^2/\omega_0^2} = 0$$

$$\sigma_a \equiv \sigma(j\omega_a), \qquad \sigma_b \equiv \sigma(j\omega_b) \tag{36}$$

For the zero-dimensional formulation of the problem of intrachamber processes, the individual peculiarities of the chamber are indirectly accounted for by the value ψ, so that it is possible to allow for some variation of the coefficient ν_k, related to it. It follows from Fig. 9 that, for a statically stable system, a dynamic instability appears when the value $\tilde{\nu}_k$ changes from $\tilde{\nu}_p$ to $L_b = L(\omega_b)$ and, consequently, ω_a changes from zero to ω_b. With $\tilde{\nu}_k > L_b$, the propellant combustion in the chamber is steady for any χ.

It is possible to show that, in the system considered, there exists a single root ω_*. For that purpose it is sufficient to vary the values ψ_u and ψ_p in such a way as to have $\tilde{\nu}_k$ varied in the range of $(\tilde{\nu}_p, L_b)$. We take $k = 1.25$. In all of the variants, the root of the denominator on the right side of Eq. (36) is less than the higher root of the numerator. Therefore, on the basis of the rules for plotting asymptotic FRFs,[13] $-\psi_k(\omega)$ and $-L_k(\omega)$ are monotonically increasing functions that give one value for ω_* when crossing $\varphi(\omega)$ and $L(\omega)$.

Figure 10 shows the stability boundaries depending on parameter variations at a pressure of 0.1 MPa. Positive values of ψ_p are chosen, which correspond to the growth of completeness of combustion with pressure. The parameter ψ_u may have a value below zero because an increase in product movement rate decreases their residence time in the combustion chamber, and increases heat transfer to the walls. With fixed values of ψ_u, a range of variations in the value of ψ_p on the stability boundary is revealed. The minimum value of ψ_p with $\chi_* = 0$ is established from the condition that $\tilde{\nu}_k = L_b$, which is obtained from Eq. (36) by means of a formal substitution of ω_a with ω_b.

The upper value of ψ_p is determined as a result of ω_* diminishing to zero and satisfying the equation $\nu_k = \nu$, which forms vertical

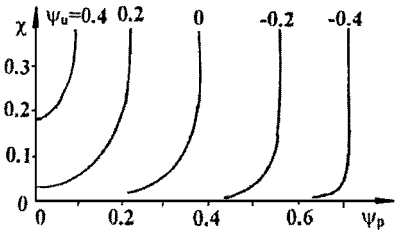

Fig. 10 Limits of stable regime depending on variation in parameters ψ_u and ψ_p at $P = 0.1$ Mpa.

asymptotes in Fig. 10. The entire configuration of the stability boundary is established by means of solving transcendental equations resulting from the equation of phases and amplitudes according to Eq. (35).

In the example considered, the differentiating properties of the TF W_p are rather limited, positive φ are small, and ω_* are close to ω_a. The curve $\chi_*(\psi_p)$ quickly approaches the asymptote in the range of small χ. Assuming that $\omega_* = \omega_a$ and discarding powers higher than the first, we obtain from the condition of the equation of phases $\varphi(\omega_a) = -\varphi_k(\omega_a)$ the approximate relationship for the stability boundary in the area of fast-changing ψ_p:

$$\chi_* = \varphi(\omega_a)/\omega_a(h_1 - h_3)$$

In Fig. 10 the stability region is located at the left of each boundary.

In case of subcritical outflow from the nozzle, the sequence of calculations remains the same. On the left-hand sides of the first two equations of system (32), the terms $z\bar{\eta}$ are added:

$$z = \frac{\mathrm{d}\ln \Gamma_0}{\mathrm{d}\ln P_0} = \frac{k-1}{2k}\left[\left(\frac{P_0}{P_e}\right)^{(k-1)/k} - 1\right]^{-1} - \frac{1}{k}$$

where P_e is external pressure, and $z > 0$ up to the transition to above-critical outflow, at which point $z = 0$. The changes touch upon the following constituent relations for Eq. (33):

$$\nu_k = \frac{2 - \psi_p + 2z}{2 + \psi_u}, \qquad h_1 = \frac{(3k+1)/k - 2\psi_p + 2z}{2 - \psi_p + 2z}$$

$$h_2 = \frac{2}{k(2 - \psi_p + 2z)}$$

From the condition $\nu_p = \nu_k$, it follows that the stability region grows because of the shift of the boundary in the direction of increasing ψ_p.

VII. Nonlinear Effects in Unsteady Burning of SPs

Accounting for nonlinear effects in the indicated region of variation in ω is the next step in describing SP unsteady burning that allows us to use the experimental data discussed in Sec. II, but this time without extrapolation to zero amplitude of the external effect.

The most convenient form for approximation of experimental data is the method of harmonic linearization of nonlinearities, which was developed in the applied theory of processes in nonlinear systems. The method was developed for practical applications in the dynamic calculations for automatic control system design.[17]

The method is unique in that the low-value parameter is introduced not into the analyzed system of nonlinear differential equations, as in the other quasi-linear methods, but directly into the solution itself.

The merits of that method include coverage of a wide class of nonlinearities, accuracy sufficient for practical purposes, ability to reveal the effect of nonlinearities even in the first approximation, ability to obtain a minimum mathematical description from the viewpoint of the number of additional dynamic parameters. Limitations include use only for oscillating systems far from initial disturbances and the need for filters in the linear portion of the automatic control system.

The equation for automatic control system dynamics is written in the form

$$Q(p)x(t) + R(p)y(t) = s(p)f(t) \tag{37}$$

Mathematical interpretation of the harmonic linearization method is reflected most simply in symmetric free oscillations when uniform equations resulting from Eq. (37) are subject to solution. Then,[17]

$$x(t) = x_1(t) + \varepsilon z(t), \qquad x_1(t) = A_1 \sin \Omega_1 t$$

$$y(t) = F(x_1, px_1) + \varepsilon\Phi(t) \tag{38}$$

After a number of transformations, the given nonlinear function is presented in the following form:

$$y = F_0 + C_1 \sin\Omega_1 + B_1 \cos\Omega_1 t + \sum_{k=2}^{\infty} F_k(t)$$

where $F_k(t)$ is the finite higher harmonics and $\varepsilon\Phi(t)$ are the small numbers of all frequencies.

For the first approximation $x = A\sin\Omega t$, the uniform equation can be transformed into a harmonically linearized one:

$$\{Q(p) + R(p)[q + (q'/\Omega)p]\}x = 0 \tag{39}$$

where q and q' are the coefficients of harmonic linearization, with

$$q = \frac{C_1}{A} = \frac{1}{\pi A}\int_0^{2\pi} F(A\sin\psi, A\Omega\cos\psi)\sin\psi\,\mathrm{d}\psi$$

$$q' = \frac{B_1}{A} = \frac{1}{\pi A}\int_0^{2\pi} F(A\sin\psi, A\Omega\cos\psi)\cos\psi\,\mathrm{d}\psi \tag{40}$$

An additional relationship,

$$\left|\frac{R(jk\Omega)}{Q(jk\Omega)}\right| = \varepsilon^n c_k \left|\frac{R(j\Omega)}{Q(j\Omega)}\right|, \qquad n \geq 1 \tag{41}$$

where c_k are the random finite positive numbers, matches the filters of the linear portion of the automatic control system so that a solution in the form of Eq. (38) is possible.

Application of the approximation method to unsteady burning-rate measurements for SPs requires consideration of the peculiarities of concrete experimental realizations.

Returning to Fig. 2, we can see that the unsteady component $u_n = u - u_q$, beginning from its maximum value, decreases in oscillating one-frequency transition regime. The filter of system linear portion operates in such a way. We can state that smoothing of high-frequency constituents is connected, to a certain degree, to the measurement method, which provides for discrete in time measurements of the sample mass with subsequent smoothing of dependencies by splines and differentiation over time. Thus, averaging of the unsteady burning rate for the sample surface is carried out automatically.

To determine the mathematical form for presentation of approximating relations, let us direct attention to the nonlinear equation of heat conductivity in the c-phase of the burning propellant, which is responsible for the character of the transition process. Let us use the simplest variant corresponding to Novozhilov's model:

$$\frac{\partial\theta}{\partial\tau} = \frac{\partial^2\theta}{\partial\xi^2} - v\frac{\partial\theta}{\partial\xi}$$

$$\xi \to -\infty, \quad \theta \to 0; \quad \xi = 0, \quad \theta = \theta_s \tag{42}$$

After finding the first integral of Eq. (42) and isolating the linear constituents, we obtain

$$\frac{\mathrm{d}}{\mathrm{d}\tau}\int_{-\infty}^{0} \theta_n\,\mathrm{d}\xi = \varphi_{Sn} - \theta_{Sn} - V_n - V_n\theta_{Sn} \tag{43}$$

Comparing Eq. (43) with the linear TF, we obtain the following operational form:

$$\left(p + c_1 - d_1\sqrt{p + \tfrac{1}{4}}\right)V_n + G(\sigma)V_n^2 = 0$$

$$c_1 = \tfrac{1}{4} + \sqrt{\tfrac{1}{16} - \lambda_0/2 + \omega_0^2}, \qquad d_1 = \sqrt{2(c - \lambda_0)}$$

$$G(\sigma) = g + h\sigma + \cdots \tag{44}$$

By excluding irrationality in the first term of Eq. (44), we get the uniform equation of dynamics,

$$\left(p^2 + 2\lambda_0 p + \omega_0^2\right)V_n + \left(p + c_1 + d_1\sqrt{p + \tfrac{1}{4}}\right)G(\sigma)V_n^2 = 0 \tag{45}$$

Note that the operational polynomial $Q(p)$ of the linear term corresponds to the TF denominator with accuracy up to the factor in (20).

It is possible to reduce operational expressions in Eq. (45) to the canonical automatic control system form if the first terms of factor expansions by p are used in the second component:

$$Q(p)v_n + R(p)F(v_n) = 0 \tag{46}$$

$$Q(p) = p^2 + 2\lambda_0 p + \omega_0^2$$

$$R(p) \cong [p(1 + d) + c_1 + d_1/2](g + hp); \qquad F(v_n) = v_n^2 \tag{47}$$

In the transition process with nonsymmetric oscillations like the process of variation in unsteady burning rate during pressure drop from an upper to a lower level, the dependence $v_n(\tau)$ is approximated in form

$$v_n = v_{n0}(\tau) + A(\tau)\sin\Psi(\tau)$$

$$\frac{dA}{d\tau} = -A\lambda(A), \qquad \frac{d\Psi}{d\tau} = \Omega(A) \tag{48}$$

Performing the harmonic linearization of Eq. (46), we obtain

$$\{Q(p) + R(p)[q + (q'/\Omega)p]\}V_n = 0 \tag{49}$$

Coefficients of harmonic linearization q and q' are determined according to Ref. 17 with the help of the relations

$$q = \frac{1}{\pi A}\int_0^{2\pi}(V_{n0} + A\sin\Psi)^2\sin\Psi\, d\Psi = 2v_{n0}^2$$

$$q' = \frac{1}{\pi A}\int_0^{2\pi}(V_{n0} + A\sin\Psi)^2\cos\Psi\, d\Psi = \frac{4v_{n0}^2}{\pi} \tag{50}$$

Depending on the amplitude, the aperiodic component v_{n0} is found from

$$Q(0)v_{n0} + R(0)F_0 = 0$$

if

$$F_0 = \frac{1}{2\pi}\int_0^{2\pi}(V_{n0} + A\sin\Psi)^2\, d\Psi = V_{n0}^2 + \frac{A^2}{2}$$

and is determined by the relation

$$V_{n0} \cong -n_u A^2, \qquad n_u = g\frac{c_1 + d_1/2}{2\omega_0^2} \tag{51}$$

After substitution of $p = -\lambda + j\Omega$ into Eq. (49) with consideration for Eqs. (50) and (51), we get two equations for actual and linear components, the solution of which gives

$$\lambda = \lambda_0 - n_\lambda A^2, \qquad \Omega = \Omega_0 - n_\omega A^2 \tag{52}$$

with

$$n_\lambda = n_u(\pi E - 4D/\pi), \qquad n_\omega = n_u(D - E)$$

$$D = (1/\Omega_0)\left\{g[c_1 + d_1/2 - \lambda_0(1 + d)] + h(1 + d_1)\Omega_0^2\right\}$$

$$E = (2/\pi)(1 + d_1)(g - 2\lambda_0 h), \qquad \Omega_0 = \sqrt{\omega_0^2 - \lambda_0^2}$$

Thus, even in the first approximation, we get corrections to the decrement of damping and frequency proportional to the square of the amplitude. They should be introduced in the expression for transfer function (26) with high unsteady burning rate deviations from the quasi-steady value. The introduced values g and h can be considered as additional dynamic parameters that determine those corrections.[18]

As additional dynamic parameters instead of g and h, any pair from among the factors n, n_λ, and n_ω can be used, given in relations (51) and (52). Their values for DB SPs are given in Table 2.

Values for n_u, n_λ, and n_ω are found as a result of processing the same experiments in which the parameters in Eq. (26) are determined, but now without extrapolation to the zero external effect.[18] Note, however, that only the results of experiments in which the transition processes from the upper level to the lower level of pressure took place were used. For that reason the possible hysteresis phenomena, which can be established by comparison with experimental data obtained during the pressure rise, were not revealed.

Thus, two additional dynamic parameters g, h or any pair from among n_u, n_λ, and n_ω allow us to account, with accuracy satisfactory for harmonic linearization, for nonlinear effects causing the dependence of the damping decrement, the oscillation frequency, and the nonoscillating constituent on the oscillation amplitude. In that sense, the complete nomenclature of dynamic parameters includes seven values: ν_p, λ_0, ω_0, a_1, a_2, and, for example, n_λ, and n_ω.

Figures 11 and 12 show a diagram of the quality of nonlinear oscillation damping for the SP studied. In the plane of the relative amplitude A-parameter (equivalent to pressure P), the lines of equal dimensional values of the damping decrement λ_d (Fig. 11)

Table 2 Values of parameters determining the corrections proportional to A^2 for linear TF

P, MPa	g	$-h$	n_u	$-n_\lambda$	n_ω
0.4	1.6	2.25	0.28	18.0	2.7
0.8	0.96	2.1	0.30	7.6	1.6
1.2	0.72	1.17	0.33	3.8	0.98
2.0	0.56	0.65	0.36	2.2	0.62
3.2	0.36	0.19	0.40	0.67	0.14
4.6	0.30	0	0.45	0.33	0.03

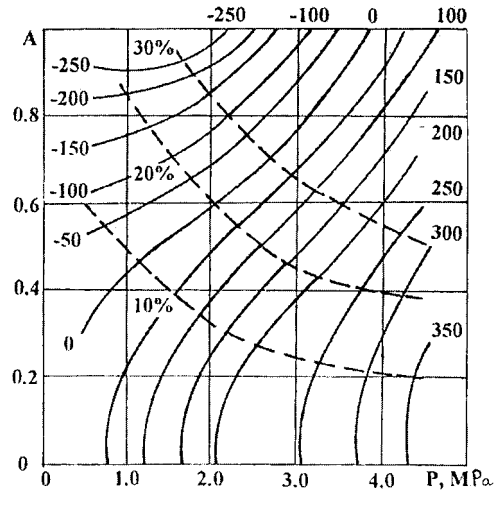

Fig. 11 Levels of dimensional fading decrement of nonlinear unsteady burning rate λ_d on the plane (A, P) for a DB propellant.

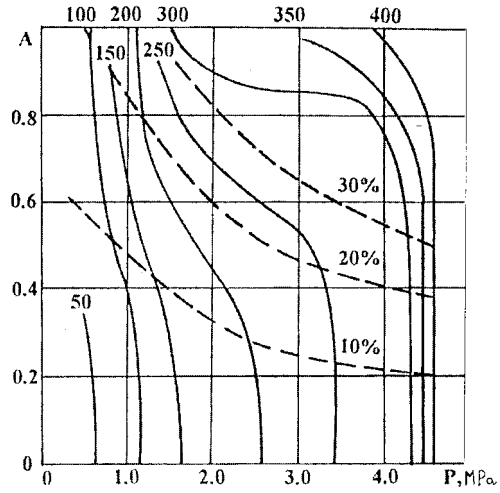

Fig. 12 Levels of dimensional fading decrement of nonlinear unsteady burning rate oscillations Ω_d on the plane (A, P) for a DB propellant.

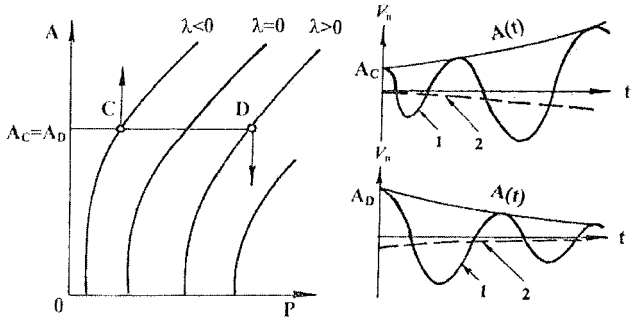

Fig. 13 Qualitative sketch of nonlinear oscillations of SP burning rate with aperiodic part: curve 1 = $\nu_n(t)$; 2 = $\nu_{n_0}(t)$.

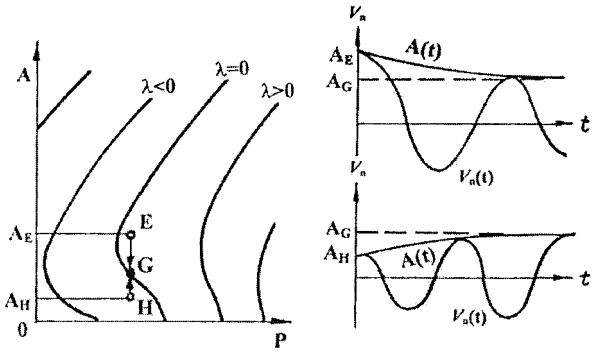

Fig. 14 Qualitative sketch of transition to self-sustained oscillatory regime in dependence of initial conditions.

and frequencies Ω_d (Fig. 12) are plotted. The dashed lines are used to mark the error values (10%, 20%, 30%) due to extrapolation of the results into the region of high amplitude values.

The quantitative picture of realization of nonlinear unsteady-burning-rate oscillations for the SP studied is shown in Fig. 13. With assigned initial relative amplitude A_c in the region of low pressure, where $\lambda < 0$ (point C), the unsteady regime with amplitude increasing over time (shown with arrow) is realized. With the same value A_D in the regime of higher pressures (point D), the regime of nonlinear oscillations is steady. In both cases the oscillations are nonsymmetrical, the nonsymmetrical constituent $v_{n0}(\tau)$ is negative.

For other SPs, for which we observe self-sustained oscillations during combustion of the unsteady burning rate a possible mechanism is shown in Fig.14. The system reaches the regime of self-sustained oscillations from the steady-state (point E) or unsteady (Point H) regime.

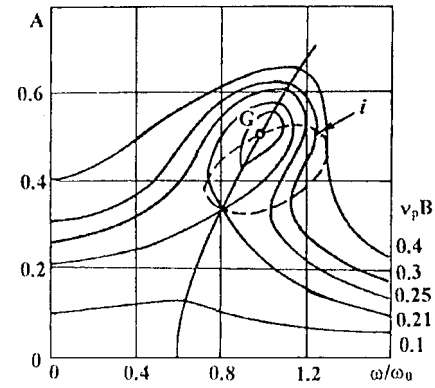

Fig. 15 Resonance curves plotted with extrapolation of experimental data into the area of large-amplitude nonlinear oscillations for a DB propellant ($P = 1.2$ MPa). Point G corresponds to a self-sustained oscillatory regime.

When studying forced oscillations of the nonsteady burning rate caused by harmonic oscillations of the external factor (pressure) with relative amplitude B, it is possible to use TF (2) subject to dependence λ_0 and ω_0 on amplitude. Then, extrapolation of the results obtained for the entire region of relative amplitude and frequency variations for the propellant studied gives the picture presented in Fig. 15. It can be seen that the resonance curves characteristic of nonsteady burning nonlinear oscillations are realized, with the derivatives $\partial A/\partial\omega$ on the curve i being infinite. A quantitative analysis of similar data is given in Ref. 2.

VIII. Conclusions

The frequency method for measuring the SP unsteady burning rate with variable external effect allows us to obtain experimental material in the form of realizations of unsteady burning rate over time, which is used for construction of functional SP unsteady burning models by methods based on automatic control theory. Low-frequency constituents of unsteady burning rate were studied, and averaging the burning surface of DB and composite SP samples was applied. It was shown that the most convenient forms for presentation of linear TFs in functional modeling are structures built on the basis of unsteady burning phenomenological theory. With help of five dynamic parameters determined as a result of experimental data processing, it is possible to solve all principal problems of SP unsteady burning linear theory. To account for nonlinear effects, it is sufficient in the first approximation to have two additional parameters obtained as a result of experimental data processing by the method of harmonic linearization.

References

[1]Zeldovich, Ya. B., "Theory of Propellant and Explosive Substance Burning," *Zhurnal Eksperimental´noi i Teoreticheskoi Fiziki* [Soviet Physics—JETP], Vol. 12, No. 12, 1942, pp. 498–509 (in Russian).

[2]Novozhilov, B. V., *Nonstationary Combustion of Solid Rocket Fuels*, Nauka, Moscow, 1973 (translation AFSC FTD-MT-24-317-74).

[3]Romanov, O. Ya., "Propellant Nonsteady Burning Rate," *Combustion, Explosion and Shock Waves (USSR)*, Vol. 11, No. 2, 1975, pp. 188–198.

[4]Denison, M. R., and Baum, E., "A Simplified Model of Unstable Burning in Solid Propellants," *ARS Journal*, Vol. 31, 1961, pp. 1112–1122.

[5]Krier, H., T´ien, J. S., Sirignano, W. A., and Summerfield, M., "Nonsteady Burning Phenomena of Solid Propellants: Theory and Experiments," *AIAA Journal*, Vol. 6, No. 2, 1968, pp. 278–285.

[6]DeLuca, L., "Theory of Nonsteady Burning and Combustion Stability of Solid Propellants by Flame Models," *Nonsteady Burning and Combustion Stability of Solid Propellants*, edited by L. DeLuca, E. W. Price, and M. Summerfield, Progress in Astronautics and Aeronautics, AIAA, Washington, DC, 1992, pp. 519–660.

[7]Bobiljev, V. M., "Investigation of Solid Propellant Nonsteady Burning as a Closed Dynamic System," *Combustion, Explosion and Shock Waves (USSR)*, Vol. 6, No. 4, 1970, pp. 454–464.

[8]Romanov, O. Ya., and Tarkchov, V. S., "Dynamic Parameters of Nonsteady Mass Burning Rate of Condensed Substance," *Combustion, Explosion and Shock Waves (USSR)*, Vol. 21, No. 4, 1986, pp. 3–11.

[9]Marchenco, V. V., Romanov, O. Ya., and Shelukhin, G. G., "Ignition and Initial Burning Period of Double-Base Propellant in a Channel," *Combustion, Explosion and Shock Waves (USSR)*, Vol. 11, No. 4, 1975, pp. 519–530.

[10]Belov, V. P., Buldakov, V. F., and Shelukhin, G. G., "Experimental Investigation of Condensed Systems' Burning Processes," *Combustion, Explosion and Shock Waves (USSR)*, Vol. 5, No. 1, 1969, pp. 42–51.

[11]Romanov, O. Ya., Tarkchov, V. S., and Shelukhin, G. G., "Measurement of Condensed Substance Nonsteady Burning Rate by the Frequency Method," *Combustion, Explosion and Shock Waves (USSR)*, Vol. 13, No. 6, 1977, pp. 924–926.

[12]Zarko, V. E., Simonenko, V. N., and Kutsenogy, K. P., "Radiant Flux Influence to Nonsteady Burning Rate in Transient Processes," *Combustion, Explosion and Shock Waves (USSR)*, Vol. 11, No. 4, 1975, pp. 541–548.

[13]Besekersky, V. A., and Popov, E. P., *Theory of Automatic Control Systems*, Nauka, Moscow, 1966 (in Russian).

[14]Ditkin, V. A., and Prudnikov, A. P., *Operatoral Theory Handbook*, Vishaya Shcola, Moscow, 1965 (in Russian).

[15]Romanov, O. Ya., and Tarkchov, V. S., "Dynamics Parameters' Application in Condensed Substances' Nonsteady Burning Tasks," *Combustion, Explosion and Shock Waves (USSR)*, Vol. 21, No. 5, 1986, pp. 27–33.

[16]Raysberg, B. A., Erochin, B. T., and Samsonov, K. P., *Theory of Operating Processes in Solid Propellants' Rocket Systems*, Mashinosroenije, Moscow, 1972 (in Russian).

[17]Popov, E. P., *Applied Theory of Automatic Control Processes in Nonlinear Systems*, Fizmathgiz, Moscow, 1973 (in Russian).

[18]Romanov, O. Ya., "Dynamic Parameters of Solid Propellant Burning with Nonlinear Effects' Consideration," *Proceedings of International Conference on Combustion*, ICOC-96, Inst. of Mechanic Problems, Izhevsk, Russia, 1997 (in Russian).